High frequency new particle formation in the Himalayas

Hervé Venzac*, Karine Sellegri*, Paolo Laj*†‡, Paolo Villani*, Paolo Bonasoni†, Angela Marinoni†, Paolo Cristofanelli†, Francescopiero Calzolari†, Sandro Fuzzi†, Stefano Decesari†, Maria-Cristina Facchini†, Elisa Vuillermoz§, and Gian Pietro Verza§

*Laboratoire de Météorologie Physique, Observatoire de Physique du Globe de Clermont-Ferrand, Université Blaise Pascal, 24 avenue des Landais, 63177 Aubière, France; †Consiglio Nazionale delle Ricerche, Institute for Atmospheric Sciences and Climate, via Gobetti 101 I-40129 Bologna, Italy; and §Ev-K2-Consiglio Nazionale delle Ricerche, via San Bernardino 145 24126 Bergamo, Italy

Edited by Veerabhadran Ramanathan, University of California at San Diego, La Jolla, CA, and approved September 3, 2008 (received for review February 13, 2008)

Rising air pollution levels in South Asia will have worldwide environmental consequences. Transport of pollutants from the densely populated regions of India, Pakistan, China, and Nepal to the Himalayas may lead to substantial radiative forcing in South Asia with potential effects on the monsoon circulation and, hence, on regional climate and hydrological cycles, as well as to dramatic impacts on glacier retreat. An improved description of particulate sources is needed to constrain the simulation of future regional climate changes. Here, the first evidence of very frequent new particle formation events occurring up to high altitudes is presented. A 16-month record of aerosol size distribution from the Nepal Climate Observatory at Pyramid (Nepal, 5,079 m above sea level), the highest atmospheric research station, is shown. Aerosol concentrations are driven by intense ultrafine particle events occurring on >35% of the days at the interface between clean tropospheric air and the more polluted air rising from the valleys. During a pilot study, we observed a significant increase of ion cluster concentrations with the onset of new particle formation events. The ion clusters rapidly grew to a 10-nm size within a few hours, confirming, thus, that *in situ* nucleation takes place up to high altitudes. The initiation of the new particle events coincides with the shift from free tropospheric downslope winds to thermal upslope winds from the valley in the morning hours. The new particle formation events represent a very significant additional source of particles possibly injected into the free troposphere by thermal winds.

aerosols | high altitude | nucleation | free troposphere

A better understanding of aerosol sources and their variability is needed for predicting the future evolution of the Earth's climate. In particular, the formation of secondary particles through nucleation of their gaseous precursors is not well constrained although it potentially represents a significant source in specific areas of the troposphere (1). This is because new particle formation is a complex process that depends on the nature of gaseous precursor species, which differ according to the environment (2, 3); on meteorological factors such as UV-radiation, temperature, and relative humidity (4); and on boundary layer dynamics (1). Thanks to recent advances in measurement techniques, new particle formation has now been observed in rural, marine, urban, and background environments (see ref. 5 for a review). However, the spatial extent of new particle formation events, in particular, their occurrence at high altitude, has rarely been documented on a long-term basis. Elevated concentrations of ultrafine particles have sporadically been observed during airborne campaigns (6, 7), and over longer time periods during ground-based measurements at the high-altitude stations of Izana [3,200 m above sea level (asl), Canary Islands] (8), and Jungfraujoch (3,580 m asl, Switzerland) (9). Although quite scarce, these studies provided indications that the process of new particle formation may not only be surface-linked, but may constitute an entire atmospheric column. However, they did not allow differentiation between *in situ* nucleation of new particles and transport of newly formed particles from the boundary layer. From a unique dataset of particle size distributions gathered over a 16-month period at the 5,079 m asl Himalayan Nepal Climate Observatory at Pyramid (NCO-P) site (10) in the Khumbu Valley, coupled with additional measurements of ions clusters performed over a two-week pilot study, this article shows that new ultrafine particle formation at high altitudes takes place very frequently, preceded by *in situ* nucleation observed during the pilot study. This process may, therefore, represent a significant source controlling the aerosol number concentration in the free troposphere throughout the whole year and may lead to substantial radiative forcing in South Asia with potential effects on the monsoon circulation (11) and, hence, on regional climate and hydrological cycles (12), as well as dramatic impacts on glacier retreat (13).

Experimental Results and Discussion. Measurements of aerosol-size distributions at the *NCO-P site* were continuously performed by using the scanning mobility particles sizer (SMPS) technique (see *Methods*). The mean diurnal variation of the particle size distribution (diameter d_p in the range of 10–700 nm), including all 511 days of observation, was calculated for each of the four distinct periods related to monsoon circulation: premonsoon (April–June), monsoon (July–September), postmonsoon (October–December), and dry (January–March) seasons (Fig. 1). The dataset is available at http://www.rrcap.unep.org/abc/data/abc/index.html. The variability of the diurnal size distribution (relative standard deviation of the mean) is available [see supporting information (SI) Fig. S1]. To our knowledge, this database represents the first long-term record of particle size distribution at >4,000 m asl. Night-time number concentration of particles [from 03:00 to 08:00 local time (LT)] are relatively constant throughout the year (560 ± 160 no. cm^{-3}), indicating the free-tropospheric background. For all seasons, the aerosol number concentration shows a clear enhancement ≈9:00 LT. The observed concentrations are surprisingly high for this high

Author contributions: P.L., P.B., and S.F. designed research; H.V., P.L., P.V., F.C., E.V., and G.P.V. performed research; H.V., K.S., P.L., A.M., P.C., S.D., and M.-C.F. analyzed data; and H.V., K.S., P.L., S.F., S.D., and M.-C.F. wrote the paper.

The authors declare no conflict of interest.

This article is a PNAS Direct Submission.

Freely available online through the PNAS open access option.

‡To whom correspondence should be addressed at: Laboratoire de Glaciologie et Géophysique de l'Environnement, Observatoire de Sciences de l'Univers de Grenoble, Université Joseph Fourier, BP 53-38041 Grenoble Cedex 9, France. E-mail: P.Laj@opgc.univ-bpclermont.fr.

This article contains supporting information online at www.pnas.org/cgi/content/full/0801355105/DCSupplemental.

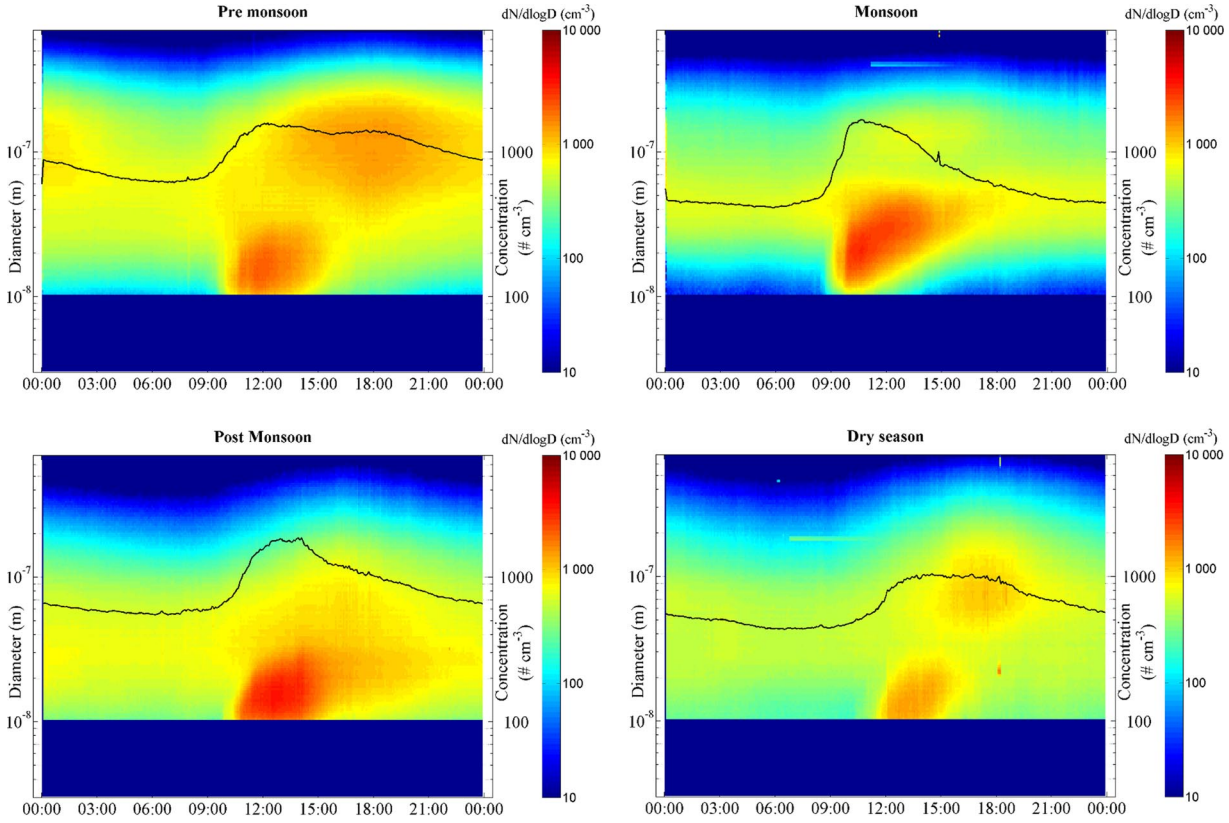

Fig. 1. Mean diurnal variation of the aerosol size distribution detected from 10 to 700 nm and total concentration (black line, right axis), averaged for the four seasons: Premonsoon, monsoon, postmonsoon, and dry season.

altitude with a mean seasonal value peaking at 2,000 no. cm^{-3} during the postmonsoon season at noontime.

For comparison, monthly averaged concentrations at the free tropospheric site of Jungfraujoch are $<$1,000 no. cm^{-3} independent of the season (9). As seen in Fig. 1, at the onset of the particle concentration increase, the aerosol population lies in the ultrafine size range (d_p of 10 nm or less). It grows in size over late morning and early afternoon hours and reaches 30–40 nm, that is, the nominal size of the Aitken mode found at night in the free troposphere in this area. The additional peak appearing in the accumulation mode ($\approx$100 nm) during the afternoon is linked to transport from combustion sources (10). The increase of 10-nm particle concentration followed by a regular growth is indicative of ultrafine particle events. Fig. 1 includes both days with and without ultrafine particle events. Clearly, average size distribution observed at high altitude in the Himalayas is significantly driven by the occurrence of ultrafine particle events. It should be noted that the simultaneous appearance of ultrafine particle events and increase in accumulation mode particle concentration results from the averaging process and does not necessarily document the occurrence of both events during the same days. Hence, the average diurnal variation (Fig. 1) is a combination of ultrafine particle events on one hand, and nonevent days on the other, shown separately in Figs. S2 and S3.

For all seasons, the initiation of the ultrafine particle concentration increase takes place between 8:00 and 11:00 LT and corresponds with the shift in wind direction at the station from a weak downslope northeasterly breeze (prevailing at night) to a strong upslope south-southwest wind (prevailing during the day). The very constant daily pattern of the upslope/downslope circulation can be observed throughout the year, although being slightly weaker during the monsoon season. The onset of the ultrafine particle formation events, hence, coincides with the advection of valley air masses to the measurement station and varies from 9:00–10:00 LT during monsoon to 12:00–13:00 LT during the dry season.

Throughout the 511-day observation period, 200 unambiguous ultrafine particle events were detected [see Figs. S1–S3 for description of identification procedures-with a maximum of events occurring during the monsoon and postmonsoon seasons, Table 1]. During these seasons, the ultrafine particle formation frequency is close to 50%. On average, ultrafine particle events are characterized by abrupt and significant increases in the total number of particles between 10 and 20 nm (CN_{10-20}), corresponding to a 10- to 20-fold increase with respect to background CN_{10-20} (Table 1).

To our knowledge, this dataset is the first long-term analysis of ultrafine particle events at high altitude. The event frequency is higher than the few reported so far by Nishita *et al.* (14) at Mt Norikura, Japan 2,770 m asl (17% of the days over a limited period of 23 days) and Venzac *et al.* (15) at Puy de Dôme, France, 1,465 m asl (events occurred in more than one third of the analyzed days). Ultrafine particle events have been reported from high-altitude sites (8, 9, and 16), but lacking long-term statistics. The ultrafine event frequency at NCO-P is lower than in the natural marine coastal environment, the highest reported so far (17), but higher than the frequency reported in the natural environment of the boreal forest (18), and surprisingly similar to ultrafine particle events reported in urban environments (19). Our results provide an important confirmation of the relevance of ultrafine particle events to influence aerosol number concentration at high altitude.

We note four interesting features related to the ultrafine particle concentration increase.

1. The increase and following growth of the new ultrafine particle number concentration takes place during several

Table 1. Frequency of occurrence of ultrafine particle events by days, 10- to 20-nm particles concentration for nonevent days and ultrafine particles mode apparition days and mean new particle number concentration formation rate for all days (J_{10}) and for ultrafine particle events days (J_{10} ultrafine events)

Season	Event days/ total days	Most frequent time period for ultrafine events	CN_{10-20} nonevent days, no. cm^{-3}		CN_{10-20} during ultrafine events, no. cm^{-3}		J_{10}, no. cm^{-3} s^{-1}	J_{10} ultrafine events, no. cm^{-3} s^{-1}
			Mean ± standard deviation	Percentile 25/50/75	Mean ± standard deviation	Percentile 25/50/75		
Dry season	18/72 (25%)	13–14h	101 ± 102	37/70/119	1,559 ± 1,080	510/1,670/2,372	0.05	0.20
Premonsoon	66/173 (38%)	11–12h	73 ± 87	30/47/82	1,328 ± 1,435	510/871/1,860	0.06	0.14
Monsoon	84/147 (57%)	10–11h	50 ± 123	12/27/51	1,186 ± 1,270	480/825/1,433	0.11	0.19
Postmonsoon	32/67 (48%)	11–12h	102 ± 66	52/81/152	1,210 ± 1,190	348/791/1,543	0.13	0.16

hours, which indicates that the events are extended, at least, to the valley scale. Indeed, a 3- to 8-h continuous growth indicates that the events can extend over >15 km (calculated from an average wind speed of 2 m s^{-1}).

2. The occurrence of new particle formation is linked to meteorological conditions at the station. Clear-sky and cloudy conditions were identified on the basis of the ratio between measured to theoretical solar irradiance. We observe that new particle formation events are inhibited under cloudy and favored under clear-sky conditions. The frequency of ultrafine particle events is 0.44 for clear-sky conditions observed from 9:00 and 10:00 LT, whereas it is only 0.22 for cloudy conditions. However, because new particle formation does not systematically occur when sunny conditions are encountered, solar irradiance is clearly not the unique driving factor.
3. Factors such as the condensational sink (CS), which is related to the amount of surface available for semivolatile gases to condense on preexisting aerosols, plays a significant role as well. When 9:00 to 10:00 LT sunny conditions are selected, the frequency of ultrafine particle events on all measurement days is 0.49 when the CS is $<2.1 \times 10^{-3}$ s^{-1}, and 0.09 when the CS is higher than this value, respectively.
4. A marked diurnal variability of CN_{10-20} is found for days with ultrafine particle events, but not on days without events (Fig. 2). Clearly, the morning peak in particle concentration does not coincide with the maximum concentration of primary aerosol tracers, represented by the black carbon concentration (eqBC). As documented in ref.10, the eqBC concentration peak in the afternoon (14:00–16:00) shows a 4-hour delay to the CN_{10-20} peak, with the latter corresponding to the accumulation mode (≈100 nm) increase seen in Fig. 1. In the absence of ultrafine particle events, eqBC still peaks in the afternoon hours. The higher eqBC concentration during nonevent days illustrates the fact that ultrafine particle events are inhibited by higher preexisting particle concentrations. These factors strongly indicate that the increase in particle number concentration is decoupled from the primary pollution aerosols transported from the valley.

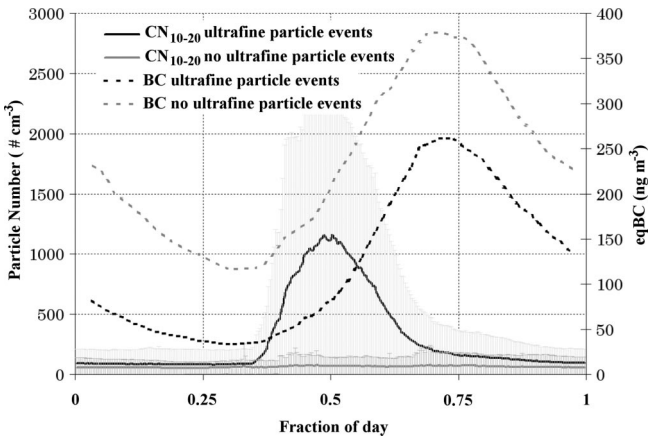

Fig. 2. Mean diurnal variation of ultrafine particles of diameter detected between 10 nm and 20 nm (plain line) and eqBC (dotted line) during days with ultrafine particle events (black, 200 days) and during days without ultrafine particle events (gray, 254 days).

The lowest particle size detected by the SMPS is 10 nm. At this size, particles may have nucleated at several tens of kilometers and traveled considerably before reaching the measurement site. Thus, it is questionable whether the nucleation process preceding the ultrafine particle events took place at the sampling site or whether it occurred in the lower valley. To provide evidence of *in situ* nucleation at this altitude, an Air Ion Spectrometer (AIS) measuring ions down to the size of 0.4 nm was installed at the station during February–March 2007. Ionic small entities can either agglomerate to clusters formed by homogeneous nucleation from gaseous precursors or represent precursors themselves. Hence, the growth of cluster ions in the 1-nm range is a proxy for particle nucleation. Cluster ions (diameter smaller than 1.4 nm) were observed to grow into larger sizes before each ultrafine particle event (detected with the SMPS) on 11 of 13 measurement days, as shown in Fig. 3.

The lifetime of such small ions can be estimated from the ion-balance equation (see *Methods*). For cluster ions to be measurable, the ion production rate from radon isotopes and cosmic rays must be higher than the ion-to-ion recombination rate and ion-aerosol attachment rate. In our case, a scale calculation results in an attachment timescale of 250 s. This means that for wind speeds of 1–3 m s^{-1}, the formation of cluster ions takes place <1 km away. Consequently, nucleation must have been initiated up to high altitudes.

Peak concentrations of 2,000 to 3,000 no. cm^{-3} cluster ions were detected on each nucleation day. Cluster ion concentrations remain very high until midafternoon. The diurnal variation of cluster ion concentrations detected at the NCO-P site has never been observed elsewhere. Contrary to other observations (20, 21), the electrical conductivity of atmospheric air associated with cluster ion concentrations does not vary with the condensational sink caused by preexisting particles, meaning that the source of ion clusters is considerably larger than their sink. The calculated source of ions shows a very strong diurnal variation with a maximum between 09:00 and 14:00 of 9 ion pair cm^{-3}. This is twice as high as the ionization rates found in the clean continental areas such as Hyytiälä (21, 22). Ion clusters, hence, are present at this high-elevation site at high enough concentrations to act as nucleation precursors and be activated as soon as condensable vapors reach a threshold limit. The subsequent apparent cluster ion growth is clear evidence that nucleation takes place everywhere in the valley as soon as photochemistry is triggered by solar radiation. Ions and particles continue to

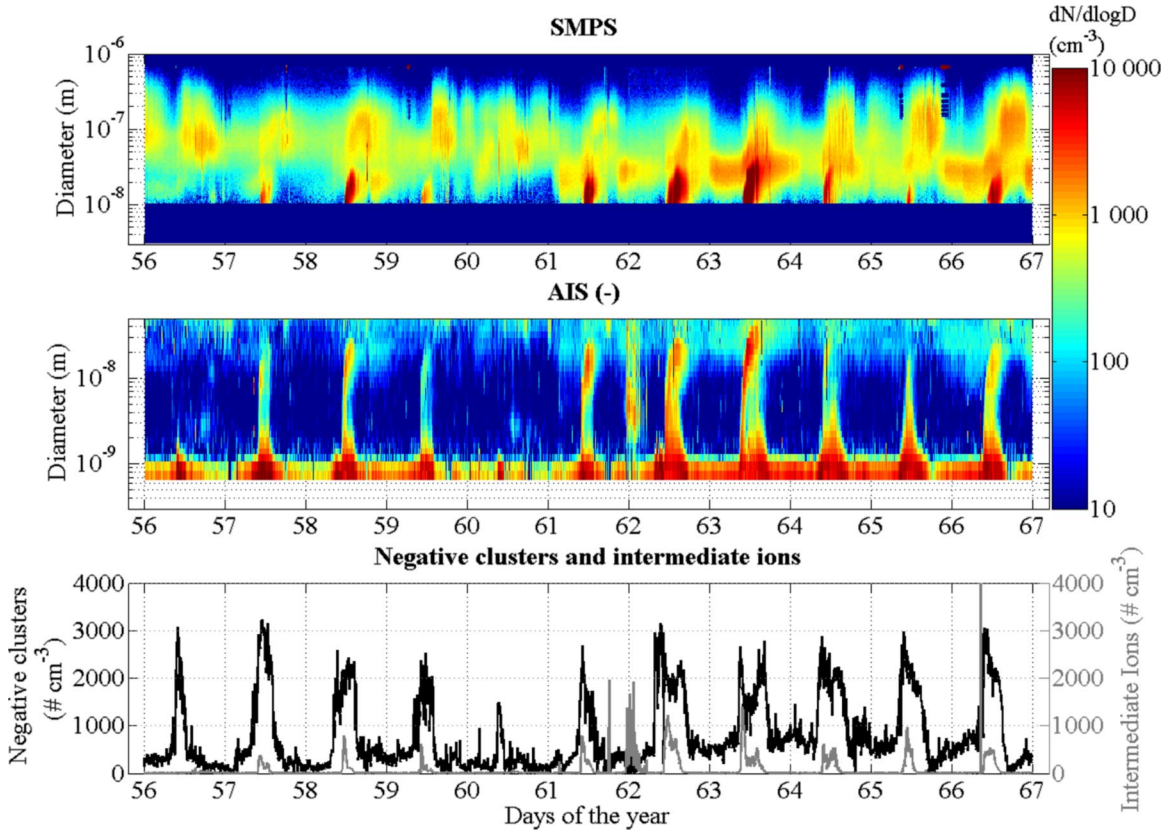

Fig. 3. Time series of the aerosol size distribution (*Top*) and ion size distribution (*Middle*) during the pilot study. *Bottom* shows the diurnal variation of the ions and charged fraction of the particles detected between 0.4 and 40 nm during a new particle formation event in March 2007.

grow throughout the day while being transported by upslope winds from locations further down in the valley where they have nucleated. During February–March 2007, stable wind conditions were encountered between 13:00 and 16:00 LT (3.8 ± 0.4 m s^{-1}, $186 \pm 5°$), allowing the calculation of a growth rate (GR). The average 3-h GR for the five clear afternoon growth events of the AIS measurement period is 1.8 ± 0.7 nm h^{-1}.

Unambiguous nucleation events were detected with the AIS during the pilot study, which was performed during the dry season. As shown in Fig. 1, daily variations of the particle concentration are similar throughout the whole year. We, therefore, think AIS results can be extended to the whole year. Our results show that very frequent *in situ* nucleation takes place at high altitude along the whole Khumbu valley. The number concentration of ultrafine particle linearly increases during the first 2 h after the onset of new particle formation events, indicating that new particle formation lasts a few hours. During this period, the new particle source rate (J_{10}) fluctuates from 0.05 (dry season) to 0.13 no. cm^{-3} s^{-1} (premonsoon) (Table 1), calculated as an average over the whole season (event and nonevent days included). When reduced to the new particle formation event days only, J_{10} is on average 0.18 no. cm^{-3} s^{-1} and maximum for the dry and monsoon seasons, corresponding to an ultrafine particle number concentration increase of 1,500 and 1,100 cm^{-3}, respectively. The cause for higher J_{10} during the monsoon and dry season may be linked to the lower preexisting aerosol background concentration previous to ultrafine particle events, as mentioned above. The apparent lower intensity of ultrafine events in Fig. 1 for dry season compared with other seasons, therefore, is due to a lower event frequency.

The vertical wind component in mountain areas plays a crucial role in transporting gases and aerosols to higher elevations. The change of air masses between day and night can be followed with the evolution of a conservative variable such as the water vapor mixing ratio (Q_v). The mixing ratio shows a clear diurnal variation with lower values during the night and maximum values in the afternoon connected to a transport of moist air from the valley. We found that nucleation (intermediate ion concentration increase) is detectable about an hour after $\Delta Q_v/dt$ changes its sign, thus, at the interface between the free troposphere and the polluted boundary layer air still containing diluted anthropogenic precursor gases. Considering that particle concentrations are locally increased by a factor of 3 or more during nucleation events which are likely taking place on a larger scale in the Himalayan valleys, new particle formation events potentially provide a significant additional source of particles to the free troposphere. Because of the very low aerosol number concentration background in the free troposphere (typically ≈550 no. cm^{-3} based on our measurements), this source may potentially control the aerosol number concentration in the free troposphere all year round. Additional modeling studies are needed to quantify the export of particle from the Himalaya valleys to the free troposphere.

The nature of the gaseous or ionic precursors involved in the new particle formation events is still unknown and will be the object of future studies. If anthropogenic precursors, possibly those emitted by domestic wood combustion, are involved in events, the predicted increase in emissions in Nepal may lead to changes of the free tropospheric aerosol background driven by both mountain slope circulation and new particle formation during upslope transport.

Methods

Aerosol and Ion Size Distribution Measurements. The NCO-P (or Nepal Climate Observatory at Pyramid) is equipped to perform continuous measurements of

chemical (organic and inorganic, soluble and insoluble), physical (PM10 mass and number size distribution), and optical (aerosol optical depth, absorption and scattering coefficients) properties of aerosols. Measurement of the light absorption coefficient by using MultiAngle Absorption Photometer is converted to equivalent Black Carbon (eqBC). In addition, measurements of reactive (O_3) and greenhouse (halocarbons) gases and meteorological parameters (wind, temperature, pressure, and surface irradiance) are performed at the station. The aerosol size distribution between 10 and 700 nm was measured with the SMPS technique by using a TSI Inc. 3010 Condensation Particle Counter (CPC) and a custom-made Differential Mobility Analyzer (DMA) (23). The data quality of the size distribution was checked by comparison of the integrated SMPS number concentration with the total concentration measured by an additional TSI Inc. 3010 CPC connected to the same sampling line. Measurements were performed at two-minute resolution from March 2006 to August 2007, with a one-month gap from August 6, 2006 to September 17, 2006 because of instrumental failure. Moreover, measurements of the charged fraction of aerosols and ion clusters down to a size of 0.4 nm were performed with an AIS (15). The AIS was operated during an intensive observation period from February 25, 2007 to March 8, 2007.

Variability of the Mean Diurnal Size Distribution of Particles. Fig. S1, shows the variability (relative standard deviation of the mean) of the mean size distribution shown in Fig. 1. The large degree of coherence (low relative standard deviation) of the size distribution in the Aitken range (30–40 nm)—not influenced by ultrafine particle events—clearly appears in the figure. This is in opposition to the large variability of the ultrafine particle events only occurring on specific days. The variability modal diameter follows the average modal diameter, which indicates that the structure of ultrafine particles events is regular and not favored at specific sizes. The variability is highest at ≈10 nm and decreases with time. The increasing diameter reflects the fact that the growth of the ultrafine particles seen in Fig. 1 is not an averaging artifact.

Identification of Ultrafine Particle Events. Three-dimensional plots of the aerosol size distribution daily variation were visually analyzed on a day-to-day basis. Each day was either classified as ultrafine particle event day or ultrafine particle nonevent day according to the criteria exposed by Dal Maso *et al.* (18). The criteria were the apparition of a clear new mode in the ultrafine size range for a substantial time period (hours) followed by a growth of these new particles to larger sizes. In our case we have used the following criteria: CN > 1,000 no. cm^{-3} above background and duration >2 h. Nevertheless, some days could not unambiguously be classified as ultrafine particle event days and were classified as ''undefined.'' The proportions of ultrafine particle event days stated in the article are consequently minimum estimates.

Ion Loss and Source Balance Scale Analysis. The ion-balance equation equals the temporal variation of ion cluster concentration with the ion production rate from radon isotopes and cosmic rays (q) minus the ion loss rate from ion-to-ion recombination ($\alpha n_{\pm} n_{\pm}$) and the ion-aerosol attachment ($n_{\pm}\beta_{\text{eff}}N_{\text{tot}}$) according to Hoppel and Frick (24):

$$\frac{dn}{dt} = q - \alpha n_{\pm} n_{\pm} - n_{\pm}\beta_{\text{eff}}N_{\text{tot}} \quad [1]$$

where $n_{\pm}$ is the number of cluster ions, α is the ion-to-ion recombination coefficient, N_{tot} is the number of aerosols, and β_{eff} is the effective ion-to-aerosol attachment coefficient. The ion sink was calculated from the ion-to-aerosol attachment coefficient (25) and the SMPS size distribution for the 9:00 to 15:00 period during the dry season. The resulting loss rate is $1 \times 10^{-3}\ s^{-1}$ for ion concentration of 2,000 ion pairs cm^{-3}. The ion-to-ion recombination coefficient α is classically used as mean value of 1.5×10^{-6} $cm^3\ s^{-1}$ derived from Hoppel and Frick (25). These scale calculations allowed us to derive an ion cluster lifetime and, for steady-state conditions, the ion cluster source rate q.

Growth Rate, Nucleation Rate, and Condensational Sink Calculation. Growth rate calculations were performed from the AIS ion size distribution obtained during the intensive February–March 2007 campaign. The growth calculation was performed for periods during which the wind direction and speed were constant, that is, from 13:00 to 16:00 LT. An ion growth was clearly detectable during this period on 5 of the 10 measurement days. The procedure comprises fitting the ion size distribution with a log-normal structure and calculating the temporal change in the modal diameter according to the method presented in Dal Maso *et al.* (18). The condensational sink is classically estimated by using sulfuric acid as a condensing molecule on the surface available from the total aerosol population according to Kulmala *et al.* (26). The formation rate of 10-nm particles was calculated from the aerosol size distribution obtained from the SMPS (10–700 nm) according to:

$$J_{10} = \frac{dCN_{10-20}}{dt} + CoagS \times CN_{10-20} \quad [2]$$

where CN_{10-20} is the number of particles detected between 10 and 20 nm and CoagS represents the sink of 10- to 20-nm particles by coagulation.

Mixing Ratio Calculation. The mixing ratio is expressed as the ratio of grams of water vapor, m_w, per kilogram of dry air, m_d, at a given pressure.

$$Qv = \frac{m_w}{m_d} = 22 \times \frac{e}{P - e}$$

where e is the partial pressure of water vapor, and P is the pressure. $e = RH \times e_{sat}/100$; e_{sat} is the water vapor to the saturated vapor pressure of water at a given temperature.

ACKNOWLEDGMENTS. This work was supported by the Italian National Research Council and the Italian Ministry of Foreign Affairs and by Centre National de la Recherche Scientifique-Institut National des Sciences de l'Univers. This study was carried out within the framework of the Ev-K^2-Consiglio Nazionale delle Ricerche Project in collaboration with the Nepal Academy of Science and Technology as foreseen by the Memorandum of Understanding between Nepal and Italy. This is a joint contribution to EU-funded Atmospheric Composition Change European Network of Excellence.

1. Spracklen D-V, *et al.* (2006) The contribution of boundary layer nucleation events to total particle concentrations on regional and global scales. *Atmos Chem Phys* 6:5631–5648.
2. O'Dowd CD, Hoffmann T (2005) Coastal new particle formation: A review of the current state-of-the-art. *Environ Chem* 2:245–255.
3. Kulmala M, Kerminen V-M, Antilla T, Laaksonen A, O'Dowd C.D (2004) Organic aerosol formation via sulfate cluster activation. *J Geophys Res*, 10.1029/2003JD003961.
4. Boy M, Kulmala M (2002) Nucleation events in the continental boundary layer: Influence of physical and meteorological parameters. *Atmos Chem Phys* 2:1–16.
5. Kulmala M, *et al.* (2004) Formation and growth rates of ultrafine atmospheric particles: A review of observations. *J Aerosol Sci* 35:143–176.
6. De Reus M (1998) Airborne aerosol measurements in the tropopause region and the dependence of new particle formation on preexisting particle number concentration. *J Geophys Res* 103:31255–31263.
7. Siebert H, Stratmann F, Wehner B (2004) First observation of increased ultrafine particle number concentrations near the inversion of a continental planetary boundary layer and ist relation to ground-based measurements. *Geophys Res Lett*, 10.1029/2003GL019086.
8. Raes F, VanDingenen R, Cuevas E, VanVelthoven P-F-J, Prospero J-M (1997) Observations of aerosols in the free troposphere and marine boundary layer of the subtropical Northeast Atlantic: Discussion of processes determining their size distribution. *J Geophys Res* 102(D17):21315–21328.
9. Weingartner E, Nyeki S, Baltensperger U (1999) Seasonal and diurnal variation of aerosol size distributions (10 < D < 750 nm) at a high-alpine site (Jungfraujoch 3580 m asl). *J Geophys Res* 104(D21):26809–26820.
10. Bonasoni P, *et al.* (2008) The ABC-Pyramid Atmospheric Research Observatory in Himalaya for aerosol, ozone and halocarbon measurements. *Sci Total Environ* 391(2–3):252–261.
11. Ramanathan V, *et al.* (2005) Atmospheric brown clouds: Impacts on South Asian climate and hydrological cycle. *Proc Natl Acad Sci USA* 102:5326–5333.
12. Ramanathan V, *et al.* (2007) Warming trends in Asia amplified by brown cloud solar absorption. *Nature* 448:575–578.
13. Flanner M-G, Zender C-S, Randerson J-T, Rasch P-J (2007) Present-day climate forcing and response from black carbon in snow. *J Geophys Res* 112:D11202,
14. Nishita C, Osada K, Kido M, Matsunaga K, Iwasaka Y (2008). Nucleation mode particles in upslope valley winds at Mount Norikura, Japan: Implications for the vertical extent of new particle formation events in the lower troposphere. *J Geophys Res* 113:D06202, 10.1029/2007JD009302.
15. Venzac H, Sellegri K, Laj P (2007) Nucleation events detected at the high altitude site of the Puy de Dôme Research Station, France. *Boreal Environ Res* 12:345–359.
16. Baltensperger U, *et al.* (1997) Aerosol climatology at the high-alpine site Jungfraujoch, Switzerland. *J Geophys Res D* 102:19707–19715.
17. Yoon Y J, O'Dowd C D, Jennings S G, and Lee S H (2006) Statistical characteristics and predictability of particle formation events at Mace Head, *J. Geophys. Res.*, 111, D13204, doi:10.1029/2005JD006284.
18. Dal Maso M, *et al.* (2005) Formation and growth of fresh atmospheric aerosols: Eight years of aerosol size distribution from SMEAR II, Hyytiälä, Finland. *Boreal Environ Res* 10:323–336.

19. Stanier C, Khlystov A, Pandis SN (2004) Nucleation events during the Pittsburgh Air Quality Study: Description and relation to key meteorological, gas phase, and aerosol parameters. *Aerosol Sci Technol* 38(S1):253–264.
20. Wilding R-J, Harrison R-G (2005) Aerosol modulation of small ion growth in coastal air. *Atmos Environ* 39:5876–5883.
21. Hõrrak U, *et al.* (2007) Characterization of positive air ions in boreal air at the Hyytiälä SMEAR station. *Atmos Chem Phys Discus* 7:9465–9517.
22. Laakso L, *et al.* (2004) Ion production rate in a boreal forest based on ion, particle and radiation measurements. *Atmos Chem Phys Discuss* 4:3947–3973.
23. Villani P, Picard D, Marchand N, Laj P (2007) Design and validation of a 6-volatility tandem differential mobility analyzer (VTDMA). *Aerosol Sci Technol* 41(10):898–906.
24. Hoppel W-A, Frick G-M (1986) Ion-aerosol attachment coefficients and the steady-state charge distribution on aerosol ion environment. *Aerosol Sci Technol* 5:1–21.
25. Hoppel W-A (1985) Ion-aerosol attachment coefficients, ion depletion, and the charge distribution on aerosols. *J Geophys Res* 90:5917–5923.
26. Kulmala M, *et al.* (2001) On the formation, growth and composition of nucleation mode particles. *Tellus* 53B:479–490.